Published in Optics Letters 4, issue 6, 1063-1070, 1987
which should be used for any reference to this work

Holographic optical scanning elements: analytical method for determining the phase function

H. P. Herzig and R. Dändliker

Institute of Microtechnology, University of Neuchatel, CH-2000 Neuchatel, Switzerland

A laser beam is deflected and focused by a holographic optical element (HOE). The hologram can be described by a phase function $\Phi(x, y)$. While displacing the HOE, the incident beam moves along a line $\mathbf{x}(s)$ in the hologram plane, and the image point describes another line $\mathbf{y}(t)$ in space. We present a method to calculate the phase function Φ, which is necessary to generate a particular line $\mathbf{y}(t)$ in space. It can be shown analytically, using second-order (paraxial) approximation, that a circular motion $\mathbf{x}(s)$ cannot generate a straight line $\mathbf{y}(t)$ in space without astigmatism of the focal spot.

1. INTRODUCTION

Holographic optical elements (HOE's) can be used as deflecting and focusing elements in laser scanners. HOE's are recorded by using spherical waves,[1] specially designed optical systems,[2] computer-generated holograms,[3] and so on. However the hologram is produced, it is possible to represent the hologram structure by a phase function $\Phi(x, y)$. In some particular cases, such as for point-of-sale systems,[4,5] simple geometrical considerations lead to the optimum recording conditions. In general the problem is more complex. One possibility for finding solutions is to use optimum design methods similar to the ones used commonly to optimize lens systems in classical optics. A merit function has to be defined that describes the scan quality, and by changing the wave-front parameters this merit function is minimized.[1,6] This method works well to find a local minimum for the special configuration admitted, but one gets little information about other solutions and the influence of the different parameters. An alternative method to determine the hologram phase function Φ analytically, first introduced by Winick and Fienup, is based on minimalization of the mean-squared wave-front error.[7,8]

In this paper we present another analytical method, which is differential rather than integral, to determine the phase function necessary to solve particular scan problems. First the basic idea is introduced and the generalized scan equation is developed. Then the theory is applied to the generation of a straight line in space by a linear and a circular motion of the HOE. The wave field generated by the HOE scanner is represented as an astigmatic pencil of rays (second-order, paraxial approximation).

2. GENERAL THEORY

A laser beam is deflected and focused by a HOE. The hologram structure can be described by a phase function $\Phi(x, y)$. While displacing the HOE, the incident beam moves along a line $\mathbf{x}(s)$ in the hologram plane, and the image point describes another line $\mathbf{y}(t)$ in space (Fig. 1). One must find the phase function $\Phi(x, y)$ that is necessary to generate a particular line $\mathbf{y}(t)$ in space.

A coordinate system u, v, w is introduced, so that the u and v axes are in the hologram plane and the w axis is normal to it. During the scan motion, this coordinate system is fixed in space, as are the incident laser beam and the generated line $\mathbf{y}(t)$. The origin of the system u, v, w is at the center of the incident laser beam in the hologram plane and on the line $\mathbf{x}(s)$. For each position t on the line $\mathbf{y}(t)$ the local phase function $\Psi(u, v, t)$ in the hologram plane can be written as

$$\Psi(u, v, t) = \Phi_p(u, v, t) - \Phi_r(u, v), \tag{1}$$

where Φ_p describes the outgoing wave, focused on the line $\mathbf{y}(t)$, and Φ_r represents the phase of the incident laser beam, which is the reconstructing reference for the hologram.

The coordinate system x, y is fixed in the hologram plane and moves with it during the scan. The incident laser beam moves in the hologram plane on the line $\mathbf{x}(s)$. At each point on $\mathbf{x}(s)$, characterized by the parameter s, the incident beam reconstructs a point on the line $\mathbf{y}(t)$, characterized by the parameter t. Therefore, within the pupil of the laser beam centered at the point s, the phase function $\Phi(x, y)$ of the hologram should be identical to the phase function $\Psi(u, v, t)$ given in Eq. (1). In general, this condition cannot be fulfilled rigorously for all points of a continuous scan. To get at least a local match of the two phase functions Φ and Ψ, these phase functions are developed in Taylor series at the point $\mathbf{x}(s)$, which corresponds to the origin of the u, v coordinate system, viz.,

$$\Phi(u, v, s) = \Phi[\mathbf{x}(s)] + \left.\frac{\partial \Phi}{\partial u_i}\right|_s u_i + \frac{1}{2}\left.\frac{\partial^2 \Phi}{\partial u_i \partial u_j}\right|_s u_i u_j + \ldots, \tag{2}$$

$$\Psi(u, v, t) = \Psi(0, 0, t) + \left.\frac{\partial \Psi}{\partial u_i}\right|_t u_i + \frac{1}{2}\left.\frac{\partial^2 \Psi}{\partial u_i \partial u_j}\right|_t u_i u_j + \ldots, \quad i, j = 1, 2. \tag{3}$$

Here and in what follows two notations are used for the components of spatial vectors, namely, $\mathbf{u} = (u, v, w) = (u_1, u_2, u_3)$, and similarly for $\mathbf{x}$ and $\boldsymbol{\xi}$.

We require now that the two series be equal up to second order, where the first-order derivatives determine the direc-

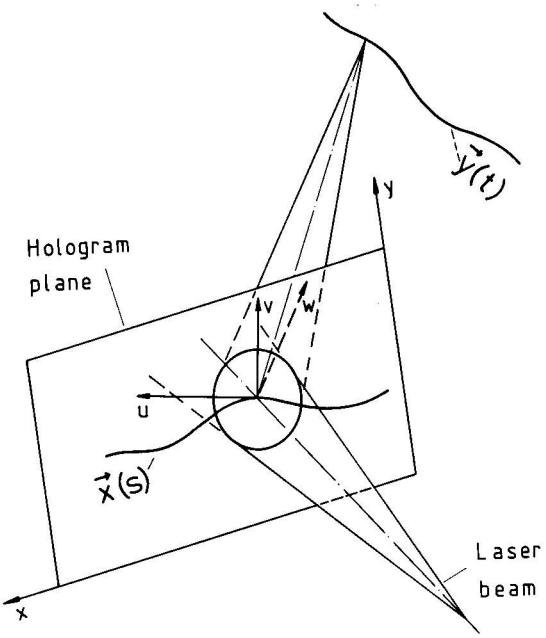

Fig. 1. General scan configuration. The hologram moves along a line $\mathbf{x}(s)$ in the hologram plane, and the image point describes another line $\mathbf{y}(t)$ in space.

tion and the second-order derivatives the curvature of the outgoing wave. This yields the following six conditions:

$$\Phi[\mathbf{x}(s)] = \Psi(0, 0, t), \tag{4}$$

$$\left.\frac{\partial\Phi}{\partial u_i}\right|_s = \left.\frac{\partial\Psi}{\partial u_i}\right|_t \equiv h_i(t), \tag{5}$$

$$\left.\frac{\partial^2\Phi}{\partial u_i \partial u_j}\right|_s = \left.\frac{\partial^2\Psi}{\partial u_i \partial u_j}\right|_t \equiv h_{ij}(t). \tag{6}$$

To find the phase function $\Phi(x, y)$, the relations between the derivatives in the two coordinate systems x, y and u, v must be established. These relations depend on the geometry of the particular scan problem. They can be formally expressed by five functions f_i and f_{ij}, namely,

$$\left.\frac{\partial\Phi}{\partial x_i}\right|_s = f_i\left(\left.\frac{\partial\Phi}{\partial u_k}\right|_s\right), \tag{7}$$

$$\left.\frac{\partial^2\Phi}{\partial x_i \partial x_j}\right|_s = f_{ij}\left(\left.\frac{\partial\Phi}{\partial u_k}\right|_s, \left.\frac{\partial^2\Phi}{\partial u_l \partial u_m}\right|_s\right). \tag{8}$$

Introducing Eqs. (5) and (6) into Eqs. (7) and (8), one obtains

$$\left.\frac{\partial\Phi}{\partial x_i}\right|_s = f_i[h_k(t)] \equiv g_i(t), \tag{9}$$

$$\left.\frac{\partial^2\Phi}{\partial x_i \partial x_j}\right|_s = f_{ij}[h_k(t), h_{lm}(t)] \equiv g_{ij}(t). \tag{10}$$

The five relations of Eqs. (9) and (10) have to be fulfilled simultaneously by the same phase function $\Phi(x, y)$ along the line $\mathbf{x}(s)$. Thus Eqs. (9) and (10) determine all possible solutions for which the outgoing wave has the desired direction and the desired curvature.

For the solution of a particular scan problem, it is necessary first to determine the functions $h_i(t)$ and $h_{ij}(t)$. They are, following Eqs. (5) and (6), equal to the first and second derivatives of the local phase function $\Psi(u, v, t)$ [Eq. (1)] required at the origin ($u = v = 0$) to focus the outgoing wave into the point t along the line $\mathbf{y}(t)$. In addition, one has to establish for the particular scan geometry the relations between the derivatives in the two coordinate systems x, y and u, v [Eqs. (7) and (8)], to obtain finally Eqs. (9) and (10) in explicit form. The value of the phase function $\Phi(x, y)$ along $\mathbf{x}(s)$ [Eq. (4)] follows by integration of Eq. (9). In Section 4 it is shown that, in general, a unique astigmatic solution can be found in this way for any particular scan problem.

3. THE SCAN EQUATION

As was mentioned above, Eqs. (9) and (10) describe all possible solutions. Of special interest is the relation between the two scan parameters s and t. If the incident laser beam falls onto the hologram with the beam center at a point s on $\mathbf{x}(s)$, it will reconstruct a well-defined point t on $\mathbf{y}(t)$; thus t is related to s. To find the scan function $t(s)$, one has to follow the evolution of the first and second derivatives of $\Phi(x, y)$ along the line $\mathbf{x}(s)$. They are given by

$$\frac{d\Phi}{ds} = \frac{\partial\Phi}{\partial x}\frac{dx}{ds} + \frac{\partial\Phi}{\partial y}\frac{dy}{ds}, \tag{11}$$

$$\frac{d^2\Phi}{ds^2} = \frac{\partial^2\Phi}{\partial x^2}\left(\frac{dx}{ds}\right)^2 + \frac{\partial^2\Phi}{\partial y \partial x}\frac{dy}{ds}\frac{dx}{ds} + \frac{\partial\Phi}{\partial x}\frac{d^2x}{ds^2} + \frac{\partial^2\Phi}{\partial y^2}\left(\frac{dy}{ds}\right)^2 + \frac{\partial^2\Phi}{\partial x \partial y}\frac{dx}{ds}\frac{dy}{ds} + \frac{\partial\Phi}{\partial y}\frac{d^2y}{ds^2}. \tag{12}$$

From Eqs. (9) and (10) one gets the following conditions for the derivatives along the line $\mathbf{x}(s)$:

$$\left.\frac{d\Phi}{ds}\right|_s = g_1(t)\frac{dx}{ds} + g_2(t)\frac{dy}{ds}, \tag{13}$$

$$\left.\frac{d^2\Phi}{ds^2}\right|_s = g_{11}(t)\left(\frac{dx}{ds}\right)^2 + g_{21}(t)\frac{dy}{ds}\frac{dx}{ds} + g_1(t)\frac{d^2x}{ds^2} + g_{22}(t)\left(\frac{dy}{ds}\right)^2 + g_{12}(t)\frac{dx}{ds}\frac{dy}{ds} + g_2(t)\frac{d^2y}{ds^2}. \tag{14}$$

Equations (13) and (14) are derivatives of the same phase function, and therefore they are not independent. The change of the first derivative along s must be equal to the second derivative, which means that

$$\frac{d}{ds}\left(\left.\frac{d\Phi}{ds}\right|_s\right) = \left.\frac{d^2\Phi}{ds^2}\right|_s. \tag{15}$$

Introducing Eqs. (13) and (14) into Eq. (15) and using $g_{12} = g_{21}$, one gets the scan equation

$$\frac{dt}{ds}\left(\frac{dg_1}{dt}\frac{dx}{ds} + \frac{dg_2}{dt}\frac{dy}{ds}\right) - g_{11}\left(\frac{dx}{ds}\right)^2 - g_{22}\left(\frac{dy}{ds}\right)^2 - 2g_{12}\frac{dx}{ds}\frac{dy}{ds} = 0, \tag{16}$$

which is a differential equation for the scan function $t(s)$. The function $t(s)$ is obtained by integration of Eq. (16) and is

therefore completely determined by the geometry of the scan problem. As a consequence, the scan motion on the line $\mathbf{x}(s)$, necessary to perform a certain scan length on the line $\mathbf{y}(t)$, is given by $t(s)$ and cannot be chosen freely.

4. HOLOGRAPHY WITH ASTIGMATIC PENCILS OF RAYS

In the approximation used above, the outgoing wave can be described as an astigmatic pencil of rays (Fig. 2). It is characterized by the direction of propagation, given by the wave vector $\mathbf{k}$, and the two focal lines at distances ρ_1 and ρ_2, respectively. This corresponds to a second-order, paraxial approximation, whereby astigmatic waves are allowed.[9] In this approximation, the optical phase is found to be

$$\Phi_p(\vec{\xi}) = \Phi_{p0} + \left(\frac{\partial \Phi_p}{\partial \xi_i}\right)\xi_i + \frac{1}{2}\left(\frac{\partial^2 \Phi_p}{\partial \xi_i \partial \xi_j}\right)\xi_i \xi_j, \qquad i,j = 1,2,3, \tag{17}$$

where $k = 2\pi/\lambda$ is the wave number and the ζ axis is chosen to be parallel to the direction of propagation, so that $(\partial \Phi_p/\partial \xi) = 0$ and $(\partial \Phi_p/\Phi\eta) = 0$. The curvature of the wave front is then described by a two-dimensional, symmetric tensor with the components $\kappa_{\xi\xi}$, $\kappa_{\xi\eta} = \kappa_{\eta\xi}$, and $\kappa_{\eta\eta}$. Its three-dimensional representation is

$$\kappa_{ij} = \frac{\partial^2 \Phi_p}{\partial \xi_i \partial \xi_j} = k \begin{bmatrix} a & c & 0 \\ c & b & 0 \\ 0 & 0 & 0 \end{bmatrix}. \tag{18}$$

Diagonalization of the tensor κ_{ij} yields the principal direction ψ and the principal radii of curvature ρ_1 and ρ_2 (Fig. 2):

$$\tan 2\psi = 2c/(a-b), \tag{19}$$

$$1/\rho_{1,2} = \tfrac{1}{2}(a+b) \pm [\tfrac{1}{2}(a-b)\cos 2\psi + c \sin 2\psi]. \tag{20}$$

From Eq. (20) the mean radius of curvature $\bar{\rho}$, i.e., the distance to the circle of least confusion, and the astigmatism A are deduced as

$$1/\bar{\rho} = \tfrac{1}{2}(1/\rho_1 + 1/\rho_2) = \tfrac{1}{2}(a+b), \tag{21}$$

$$A = \tfrac{1}{2}(1/\rho_1 - 1/\rho_2) = \tfrac{1}{2}(a-b)\cos 2\psi + c \sin 2\psi. \tag{22}$$

By using Eq. (19), the amount of astigmatism can be written differently as

$$A^2 = (a-b)^2/4 + c^2. \tag{23}$$

The phase in the hologram plane $\Psi(u, v)$ is essentially governed by the condition of phase matching, which reads as

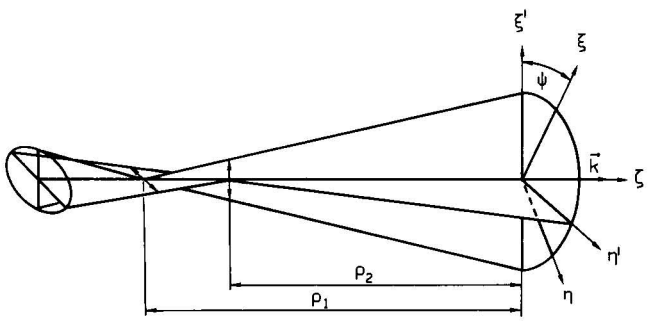

Fig. 2. Astigmatic pencil of rays.

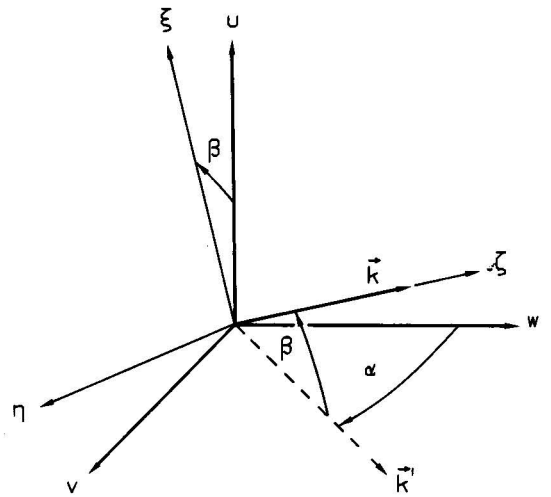

Fig. 3. Geometrical relation of the hologram plane (u, v) and a pencil of rays. The wave vector $\mathbf{k}$ is parallel to the ζ axis. $\mathbf{k}'$ is the projection of $\mathbf{k}$ onto the plane (v, w).

$$\Psi(\mathbf{u}_H) = \Phi_p(\mathbf{u}_H) - \Phi_r(\mathbf{u}_H), \tag{24}$$

where r is the reconstructing reference and p the reconstructed astigmatic wave front. Therefore the phase distribution for each pencil of rays in the hologram plane has to be calculated first. The geometrical relation of the hologram plane and the reconstructed pencil of rays is sketched in Fig. 3. The direction of propagation is given by two angles, α and β, so that the components of the wave vector $\mathbf{k}$ are

$$k_u = k \sin\beta, \qquad k_v = k \sin\alpha \cos\beta, \qquad k_w = k \cos\alpha \cos\beta, \tag{25}$$

with $-\pi/2 < \alpha < \pi/2$, $-\pi/2 < \beta < \pi/2$, and $k = 2\pi/\lambda$.

Note that the wave vector $\mathbf{k}$ is assumed to point in the positive direction of the w axis. This restriction is necessary to enable us to distinguish between divergent ($\rho > 0$) and convergent ($\rho < 0$) waves.

The transformation from the (ξ, η, ζ) to the (u, v, w) coordinates is performed by two subsequent rotations. The first is around the η axis by the angle β, and the second is then around the u axis by the angle α. The corresponding transformation matrix R is found to be

$$R = \begin{bmatrix} \cos\beta & 0 & \sin\beta \\ -\sin\alpha \sin\beta & \cos\alpha & \sin\alpha \cos\beta \\ -\cos\alpha \sin\beta & -\sin\alpha & \cos\alpha \cos\beta \end{bmatrix}. \tag{26}$$

Furthermore, the direction of the outgoing wave and the tensor of curvature have to be projected onto the hologram plane. This projection tensor P in (u, v, w) coordinates becomes

$$P = \begin{bmatrix} 1 & 0 & 0 \\ 0 & 1 & 0 \\ 0 & 0 & 0 \end{bmatrix}. \tag{27}$$

For the direction $\mathbf{m}_p$ of the outgoing wave and the tensor of curvature χ_p in the hologram plane, it then follows that

$$\mathbf{m}_p = PR\mathbf{k} = k(\sin\beta, \sin\alpha \cos\beta), \tag{28}$$

$$\chi_p = PR\kappa R^{-1}P$$

$$= k\begin{bmatrix} a\cos^2\beta & -a\sin\alpha\sin\beta\cos\beta + c\cos\alpha\cos\beta \\ -a\sin\alpha\sin\beta\cos\beta + c\cos\alpha\cos\beta & a\sin^2\alpha\sin^2\beta - 2c\sin\alpha\cos\alpha\sin\beta + b\cos^2\alpha \end{bmatrix}, \quad (29)$$

where $\mathbf{k}$ and κ are given in the (ξ, η, ζ) system and $\mathbf{m}_p$ and χ_p is in the hologram plane (u, v).

During the scan motion the direction of propagation $\mathbf{k}$ and the curvature κ of the outgoing wave will change with the scan parameter t (Fig. 1). This means that both Eqs. (28) and (29) are functions of t through $\alpha(t)$, $\beta(t)$, $a(t)$, $b(t)$, and $c(t)$. To generate a particular scan line $\mathbf{y}(t)$ in space, these functions have to be established from geometrical considerations. For a straight line $\mathbf{y}(t)$ in space, the direction of the outgoing wave remains in a plane, which can be assumed to contain the u axis of the hologram plane (Fig. 3). In this case, α is constant during the scan (α = constant), and β can be considered the scan parameter t ($\beta = t$).

The incident beam (Φ_r) can be treated in the same second-order (paraxial) approximation. It keeps its position in space during the scan motion. The direction of propagation is now characterized by the two angles γ and δ, where γ corresponds to α and δ to β in Fig. 3. We assume that the incident wave is spherical with radius ρ, which means that $a = b = 1/\rho$ and $c = 0$. Thus the direction $\mathbf{m}_r$ and the curvature χ_r of the incident wave in the hologram plane become

$$\mathbf{m}_r = k(\sin\delta, \sin\gamma\cos\delta), \quad (30)$$

$$\chi_r = \frac{k}{\rho}\begin{bmatrix} \cos^2\delta & -\sin\gamma\sin\delta\cos\delta \\ -\sin\gamma\sin\delta\cos\delta & \sin^2\gamma\sin^2\delta + \cos^2\gamma \end{bmatrix}. \quad (31)$$

Using the relations of Eqs. (28) to (31), the phase distribution in the hologram plane can be calculated up to second order from

$$\Psi(\mathbf{u}_H, t) = \Psi_0 + \mathbf{m}^T\mathbf{u}_H + \tfrac{1}{2}\mathbf{u}_H{}^T\chi\mathbf{u}_H, \quad (32)$$

where $\mathbf{m}$ and χ are obtained from the condition of phase matching in Eq. (24). One finally obtains

$$\mathbf{m}(\mathbf{u}_H, t) = \left(\frac{\partial\Psi}{\partial u_i}\bigg|_t\right) = \mathbf{m}_p(\mathbf{u}_H, t) - \mathbf{m}_r(\mathbf{u}_H) = h_i(t), \quad (33)$$

$$\chi(\mathbf{u}_H, t) = \left(\frac{\partial^2\Psi}{\partial u_i\partial u_j}\bigg|_t\right) = \chi_p(\mathbf{u}_H, t) - \chi_r(\mathbf{u}_H) = h_{ij}(t), \quad i, j = 1, 2. \quad (34)$$

Equations (33) and (34), respectively, now describe the first and second derivatives of the local phase function $\Psi(u, v, t)$, i.e., $h_i(t)$ and $h_{ij}(t)$ in Eqs. (5) and (6).

To continue the determination of the hologram phase function $\Phi(x, y)$, the relations between the derivatives in the two coordinate systems x, y and u, v must be established. They depend on the geometry of the scan problem and in particular on the motion $\mathbf{x}(s)$ of the incident beam in the plane of the HOE scanner. In what follows, the two special cases of liner motion and circular motion are discussed in detail.

5. LINEAR MOTION

The first problem that we shall discuss is the case in which the hologram moves along a straight line $\mathbf{x}(s)$ and the outgoing wave also generates a straight line $\mathbf{y}(t)$ in space, as shown in Fig. 4. The linear motion of the hologram is assumed to be parallel to the generated line $\mathbf{y}(t)$ and parallel to the x axis, which is therefore also parallel to the u axis. In this situation, it is convenient to use x as the scan parameter s in the hologram plane ($x = s$) and the deflection angle β as the scan parameter t in space ($\beta = t$). The derivatives of Φ in the two coordinate systems x, y and u, v [Eqs. (7) and (8)] are then simply related by

$$\frac{\partial\Phi}{\partial x_i} = \frac{\partial\Phi}{\partial u_i}, \qquad \frac{\partial^2\Phi}{\partial x_i\partial x_j} = \frac{\partial^2\Phi}{\partial u_i\partial u_j}, \qquad i, j = 1, 2. \quad (35)$$

Introducing these relations into Eqs. (9) and (10), one gets for the derivatives of $\Phi(x, y)$ on the scan line $\mathbf{x}(s) = (x, y = 0)$

$$\frac{\partial\Phi}{\partial x_i}\bigg|_{y=0} = h_i(\beta), \qquad \frac{\partial^2\Phi}{\partial x_i\partial x_j}\bigg|_{y=0} = h_{ij}(\beta), \quad (36)$$

where h_i and h_{ij} are given by the local phase $\Psi(u, v, \beta)$ required for the desired outgoing wave [Eqs. (5) and (6)].

Using second-order (paraxial) approximation, the functions $h_i(\beta)$ and $h_{ij}(\beta)$ can be obtained with the help of Eqs. (33) and (34). For the scan geometry shown in Fig. 4 one gets, with $\alpha \neq 0$ and $\delta = 0$,

$$h_1 = k\sin\beta, \qquad h_2 = k(\sin\alpha\cos\beta - \sin\gamma), \quad (37)$$

$$h_{11} = k(a\cos^2\beta - 1/\rho), \quad (38a)$$

$$h_{12} = h_{21} = k(c\cos\alpha\cos\beta - a\sin\alpha\sin\beta\cos\beta), \quad (38b)$$

$$h_{22} = k(a\sin^2\alpha\sin^2\beta - 2c\sin\alpha\cos\alpha\sin\beta + b\cos^2\alpha - \cos^2\gamma/\rho). \quad (38c)$$

To get the scan equation [cf. Eqs. (15) and (16)] and the phase function $\Phi(x, y)$, one has to follow the development of $\Phi(x, y)$ along the scan line $\mathbf{x}(s) = (x, y = 0)$.

Perpendicular to the scan line, i.e., in the y direction, a second-order (parabolic) approximation of $\Phi(x, y)$ will be sufficient to satisfy Eqs. (36). Therefore the phase function may be written as

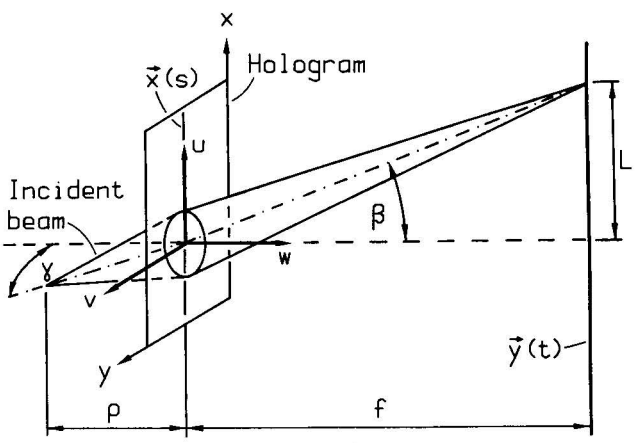

Fig. 4. Linear motion $\mathbf{x}(s)$ of the hologram to generate a straight line $\mathbf{y}(t)$.

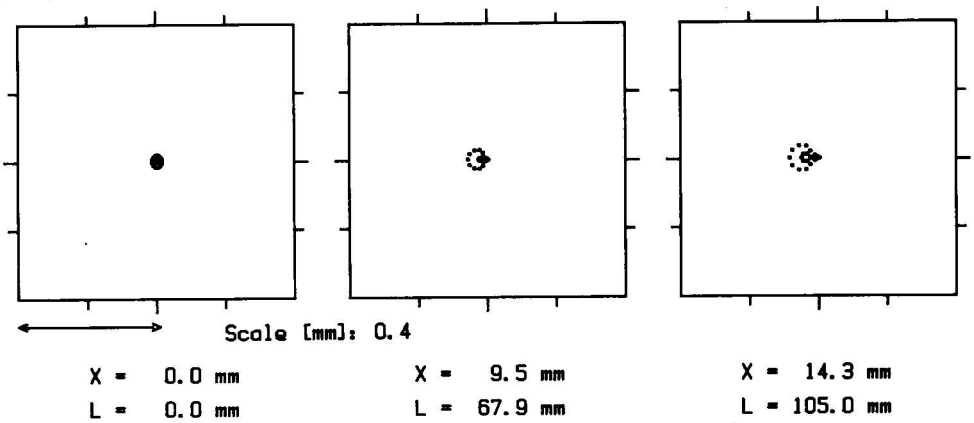

Fig. 5. Spot diagrams for three linear hologram positions x, corresponding to the scan lengths L. The geometrical parameters (Fig. 4) are f = 300 mm, D = 5 mm, ρ = 50 mm, α = 0 deg, and γ = 0 deg.

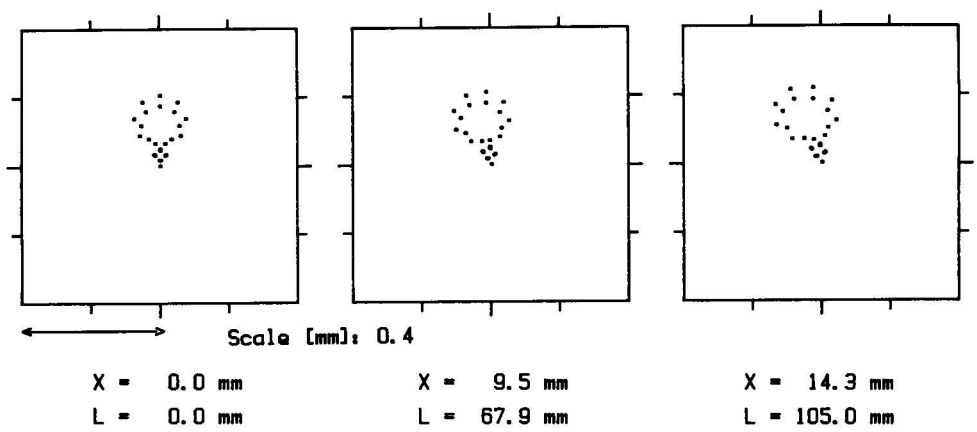

Fig. 6. Spot diagrams for three linear hologram positions x, corresponding to the scan lengths L. The geometrical parameters (Fig. 4) are f = 300 mm, D = 5 mm, ρ = 50 mm, α = 0 deg, and γ = −10 deg.

$$\Phi(x, y) = k[a_0(x) + a_1(x)y + (1/2)a_2(x)y^2]. \tag{39}$$

Applying Eqs. (36)–(38) to Eq. (39), one finally obtains

$$a_0' = \sin\beta, \qquad a_0'' = a\cos^2\beta - 1/\rho, \tag{40}$$

$$a_1 = \sin\alpha\cos\beta - \sin\gamma,$$

$$a_1' = c\cos\alpha\cos\beta - a\sin\alpha\sin\beta\cos\beta, \tag{41}$$

$$a_2 = a\sin^2\alpha\sin^2\beta - 2c\sin\alpha\cos\alpha\sin\beta + b\cos^2\alpha - \cos^2\gamma/\rho, \tag{42}$$

with $' = \mathrm{d}/\mathrm{d}x$ and $'' = \mathrm{d}^2/\mathrm{d}x^2$.

An ideally focused (spherical) outgoing wave requires that $a = b = -\cos\beta/f$ and $c = 0$, where f is the distance between the hologram and the image plane [Fig. 4].

Since the relation $a_0'' = \mathrm{d}(a_0')/\mathrm{d}x$ has to be fulfilled, one obtains from Eqs. (40) the scan equation

$$\mathrm{d}\beta/\mathrm{d}x - a(\beta)\cos\beta + 1/\rho\cos\beta = 0, \tag{43}$$

where $a(\beta) = -\cos\beta/f$. Equation (43) determines the relation $\beta(x)$ between the scan angle β and the displacement x of the hologram.

As with Eq. (43), one has to fulfill $a_1' = \mathrm{d}a_1/\mathrm{d}x$, which yields from Eqs. (41)

$$\mathrm{d}\beta/\mathrm{d}x - a(\beta)\cos\beta + c(\beta)/\tan\alpha\tan\beta = 0. \tag{44}$$

Since the scan equation (43) and Eq. (44) must be satisfied simultaneously, one gets for $c(\beta)$ the condition

$$c(\beta) = \tan\alpha\sin\beta/\rho\cos^2\beta. \tag{45}$$

As can be seen from Eq. (23), c essentially determines the astigmatism A of the outgoing wave. It becomes minimal ($|A| = |c|$) for $a = b$. This condition can be satisfied by choosing $a_2(\beta)$ from Eq. (42) accordingly. As a consequence, there remains an astigmatism $|A| = |c|$, given by Eq. (45), with the principal direction ψ = 45 deg [Eq. (19)]. The astigmatism is equal to zero for $\beta = 0$, but it is not possible to keep A equal to zero for all scan angles β, unless the incident wave is plane ($\rho = \infty$) or the scan plane is perpendicular to the hologram ($\alpha = 0$).

In summary, one finds a well-defined phase function $\Phi(x, y)$ [Eq. (39)] for the hologram, which produces in second-order (paraxial) approximation an ideally focused (spherical) wave on a straight line in space.

For a better understanding of the scan equation, it is convenient to replace the angle β by the scan length $L = f\tan\beta$ in the image plane (Fig. 4), so that Eq. (43) becomes

$$\mathrm{d}L/\mathrm{d}x = -(1 + f/\rho\cos^3\beta). \tag{46}$$

The right-hand side of Eq. (46) is the differential magnification M of the scan, namely, the ratio between the move-

ment dL of the focus on the line $\mathbf{y}(t)$ and the displacement dx of the hologram. In the case of a plane incident wave ($\rho = \infty$), one obtains $M = 1$, which means that the displacement of the hologram is equal to the scan length. If the incident wave is divergent ($\rho > 0$), one gets $M > 1$, and the displacement of the hologram becomes smaller than the scan length.

To get an idea of the real quality, including higher-order aberrations, of these second-order solutions, we have applied geometrical ray tracing to the holograms described by Eq. (39). A computer program based on Ref. 10 has been developed for that purpose. The calculations have been made for a scan-line distance $f = 300$ mm, a divergent incident beam with $\rho = 50$ mm, and a diameter $D = 5$ mm of the beam in the hologram plane (Fig. 4). To avoid astigmatism, the inclination of the scan plane is chosen to be $\alpha = 0$ [Eq. (45)]. Figures 5 and 6 show the spot diagrams for three hologram positions x with the corresponding scan lengths $L = 0$, 67.9, and 105 mm. The inclination of the incident wave is $\gamma = 0$ deg in Fig. 5 and $\gamma = -10$ deg in Fig. 6. The second case shows strong higher-order aberrations in the y direction, which are caused by the inclination of the incident beam. These aberrations perpendicular to the scan line $\mathbf{x}(s)$ could easily be corrected by introducing adequate higher-order terms $a_i(y)$ in the phase [Eq. (39)], whereas in the direction of the scan line (x direction) the aberrations are completely determined by the solution of the scan equation (43).

6. CIRCULAR MOTION

In the case of circular motion, the hologram turns around the z axis (Fig. 7); the rotation angle is ϕ. The line $\mathbf{x}(s)$ is a circle of radius R, and therefore it is convenient to use ϕ as the scan parameter s in the hologram plane ($\phi = s$). The generated line $\mathbf{y}(t)$ is again a straight line, and the deflection angle β will be used as the scan parameter t in space ($\beta = t$). The generated line is assumed to be parallel to the hologram

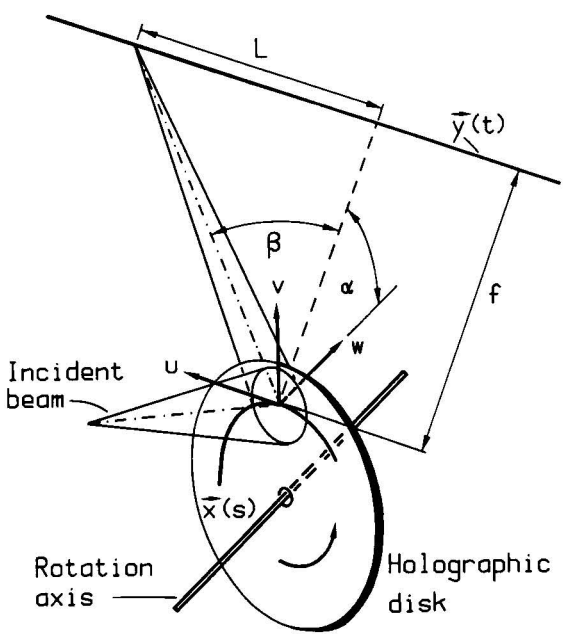

Fig. 7. Circular motion $\mathbf{x}(s)$ of the hologram (rotating disk) to generate a straight line $\mathbf{y}(t)$ in space.

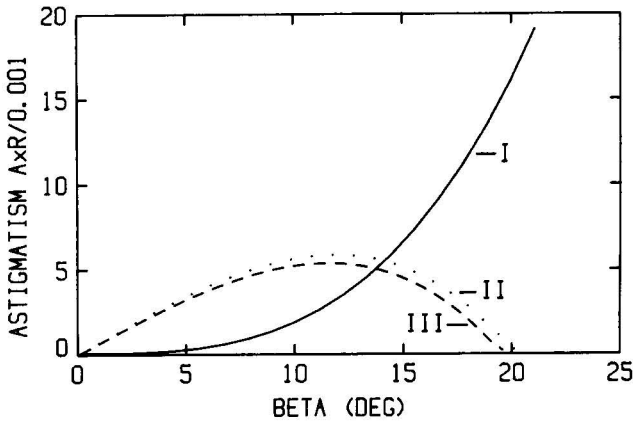

Fig. 8. Angular dependence of the astigmatism A represented by the product of $|A \times R| = |(R/2)(1/\rho_1 - 1/\rho_2)|$, where R is the disk radius. Case I, plane incident wave $\rho/R = \infty$, $\alpha = 45$ deg, $\gamma = -45$ deg. Case II, convergent incident wave $\rho/R = -25$, $\alpha = 45$ deg, $\gamma = -45$ deg. Case III, divergent incident wave $\rho/R = 1.5$, $\alpha = 45$ deg, $\gamma = 0$ deg.

plane, with the scan plane tangential to the hologram motion, which means that the u axis is tangential to the circle $\mathbf{x}(s)$ (Fig. 7). Instead of the Cartesian coordinates x, y, polar coordinates r, ϕ are introduced in the hologram plane. The derivatives of Φ in the two coordinate systems r, ϕ and u, v on the circle $\mathbf{x}(s) = (r = R, \phi)$ are then related by

$$\frac{\partial\Phi}{\partial\phi} = R\frac{\partial\Phi}{\partial u}, \qquad \frac{\partial\Phi}{\partial r} = \frac{\partial\Phi}{\partial v}, \tag{47}$$

$$\frac{\partial^2\Phi}{\partial\phi^2} = R^2\frac{\partial^2\Phi}{\partial u^2} - R\frac{\partial\Phi}{\partial v},$$

$$\frac{\partial^2\Phi}{\partial r\partial\phi} = R\frac{\partial^2\Phi}{\partial u\partial v} + \frac{\partial\Phi}{\partial u}, \qquad \frac{\partial^2\Phi}{\partial r^2} = \frac{\partial^2\Phi}{\partial v^2}. \tag{48}$$

Introducing these relations into Eqs. (9) and (10), one gets for the derivatives of $\Phi(r, \phi)$ on the scan line ($r = R$)

$$\frac{\partial\Phi}{\partial\phi} = Rh_1(\beta), \qquad \frac{\partial\Phi}{\partial r} = h_2(\beta), \tag{49}$$

$$\frac{\partial^2\Phi}{\partial\phi^2} = R^2h_{11}(\beta) - Rh_2(\beta),$$

$$\frac{\partial^2\Phi}{\partial r\partial\phi} = Rh_{12}(\beta) + h_1(\beta), \qquad \frac{\partial^2\Phi}{\partial r^2} = h_{22}(\beta), \tag{50}$$

where h_i and h_{ij} are given by the local phase $\Psi(u, v, \beta)$ required for the desired outgoing wave [Eqs. (5) and (6)].

As in the case of linear motion, we assume for the phase function $\Phi(r, \phi)$ a second-order (parabolic) approximation perpendicular to the scan line. Therefore the phase function may be written similar to Eq. (39) as

$$\Phi(r, \phi) = k[a_0(\phi) + a_1(\phi)(r - R) + (\tfrac{1}{2})a_2(\phi)(r - R)^2]. \tag{51}$$

Using a second-order (paraxial) approximation, the functions $h_i(\beta)$ and $h_{ij}(\beta)$ can be obtained with the help of Eqs. (33) and (34) for the scan geometry shown in Fig. 7 with $\delta = 0$. Introducing the results into Eqs. (49) and (50), one gets finally

$$a_0' = R \sin\beta,$$

$$a_0'' = R^2(a \cos^2\beta - 1/\rho) - R(\sin\alpha \cos\beta - \sin\gamma), \quad (52)$$

$$a_1 = \sin\alpha \cos\beta - \sin\gamma,$$

$$a_1' = \sin\beta + R(c \cos\alpha \cos\beta - a \sin\alpha \sin\beta \cos\beta), \quad (53)$$

$$a_2 = a \sin^2\alpha \sin^2\beta - 2c \sin\alpha \cos\alpha \sin\beta + b \cos^2\alpha - \cos^2\gamma/\rho, \quad (54)$$

with $' = \mathrm{d}/\mathrm{d}\phi$ and $'' = \mathrm{d}^2/\mathrm{d}\phi^2$.

Since the relation $a_0'' = \mathrm{d}(a_0')/\mathrm{d}\phi$ must be fulfilled, one obtains from Eqs. (52) the scan equation

$$\mathrm{d}\beta/\mathrm{d}\phi - Ra(\beta) \cos\beta + R/\rho \cos\beta + \sin\alpha - \sin\gamma/\cos\beta = 0, \quad (55)$$

which determines the relation $\beta(\phi)$ between the scan angle β and the rotation ϕ of the hologram for a given curvature $a(\beta)$ of the outgoing wave in the scan plane. The geometry shown in Fig. 7 requires for ideal focusing that $a(\beta) = -\cos\beta/f$, and therefore the scan equation becomes

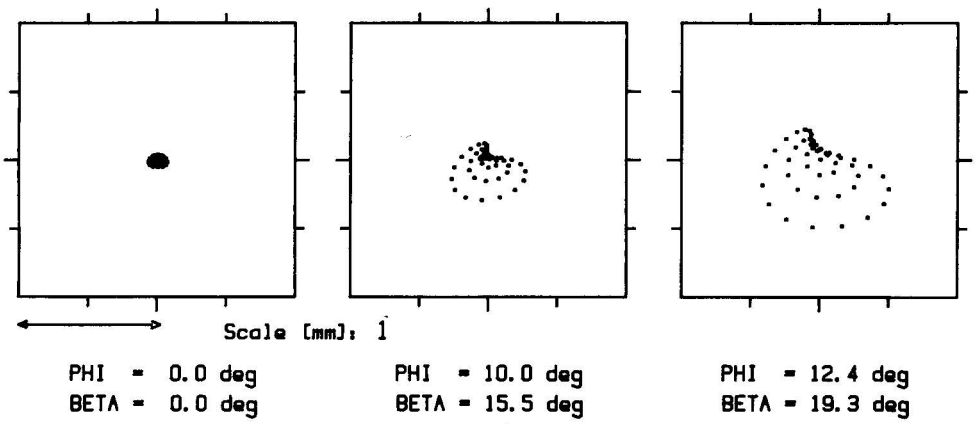

Fig. 9. Spot diagrams for three circular hologram positions ϕ, corresponding to the scan angles β. The geometrical parameters (Fig. 7) are f = 300 mm, D = 5 mm, $\rho = \infty$, α = 45 deg, γ = −45 (case I). The maximum scan length L = tan β is 105 mm.

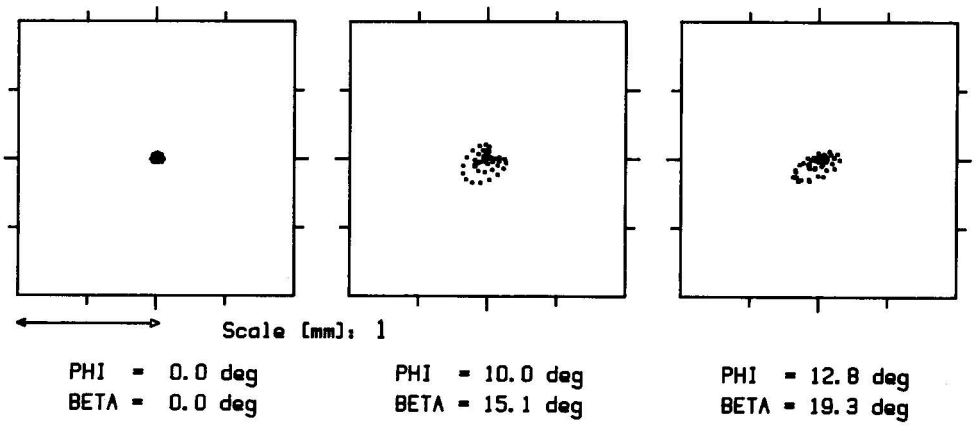

Fig. 10. Spot diagrams for three circular hologram positions ϕ, corresponding to the scan angles β. The geometrical parameters (Fig. 7) are f = 300 mm, D = 5 mm, ρ = −1000 mm, α = 45 deg, γ = −45 deg (case II). The maximum scan length L = tan β is 105 mm.

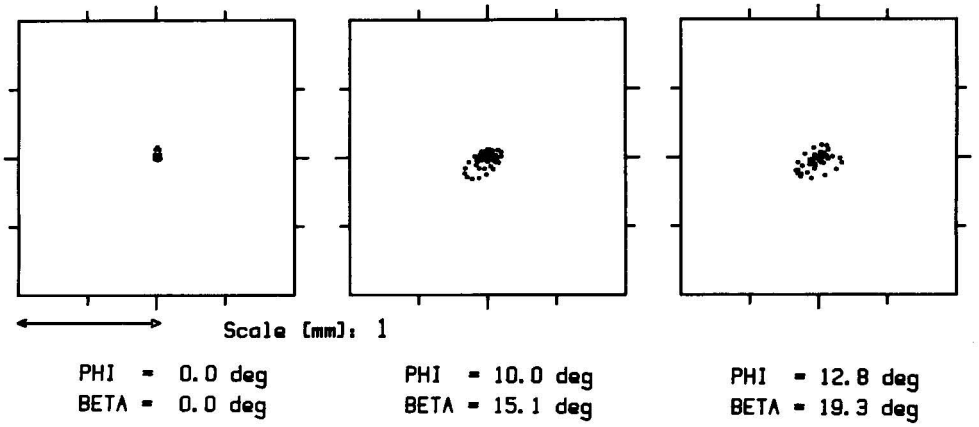

Fig. 11. Spot diagrams for three circular hologram positions ϕ, corresponding to the scan angles β. The geometrical parameters (Fig. 7) are f = 300 mm, D = 5 mm, ρ = 60 mm, α = 45 deg, γ = 0 deg (case III). The maximum scan length L = tan β is 105 mm.

$$d\beta/d\phi = R(-\cos^2\beta/f - 1/\rho\cos\beta) - \sin\alpha + \sin\gamma/\cos\beta. \quad (56)$$

As with Eq. (55), one must fulfill $a_1' = da_1/d\phi$, which yields from Eqs. (53)

$$d\beta/d\phi - Ra(\beta)\cos\beta + 1/\sin\alpha + Rc(\beta)/\tan\alpha\tan\beta = 0. \quad (57)$$

Since the scan equation (55) and Eq. (57) must be satisfied simultaneously, one gets for c the condition

$$c(\beta) = (\tan\beta/R)[(\tan\alpha/\cos\beta)(R/\rho - \sin\gamma) - \cos\alpha]. \quad (58)$$

As can be seen from Eq. (23), c essentially determines the astigmatism A of the outgoing wave. It becomes minimal ($|A| = |c|$) for $a = b$. This condition can be satisfied by choosing $a_2(\beta)$ from Eq. (54) accordingly. As a consequence, there remains an astigmatism $|A| = |c|$, given by Eq. (58), with the principal direction $\psi = 45$ deg [Eq. (19)]. The astigmatism is equal to zero for $\beta = 0$, but it is not possible to keep A equal zero for all scan angles β.

Figure 8 shows the astigmatism $A(\beta)$ as function of the scan angle β for an inclination $\alpha = 45$ deg of the scan plane. For a plane incident wave ($\rho = \infty$, $\gamma = -45$ deg, case I), the astigmatism grows continuously with the scan angle β. A better solution can be obtained if a spherical incident wave is used (case II), which compensates for the astigmatism at the end of the scan. From Eq. (58) one gets $\rho/R = -25$ for $c = 0$ at a scan angle of $\beta = 20$ deg, which corresponds to a slightly convergent incident wave. By changing the angle of the incident wave to $\gamma = 0$ deg, a similar solution is obtained for a divergent wave of $\rho/R = 1.5$ (case III). Other favorable geometries may be found from Eq. (58) to minimize the average astigmatism.

As in the case of linear motion, we have applied geometrical ray tracing to the holograms described by Eq. (51). The calculations have been made for a scan-line distance $f = 300$ mm, a beam diameter $D = 5$ mm, and a radius $R = 40$ mm in the hologram plane. Figure 9 shows the results for a plane incident wave (case I) at three positions of the holographic scanner, namely, $\phi = 0, 10, 12.4$ deg, which correspond to $\beta = 0, 15.5, 19.3$ deg, respectively. The maximum scan length in the image plane is $L = f\tan\beta = \pm 105$ mm. The arc length on the circle in the hologram plane used for that scan is only ± 8.6 mm, which is quite small compared with the beam diameter $D = 5$ mm. Therefore the higher-order aberrations revealed by the ray tracing are expected to be considerable. Figures 10 and 11 show spot diagrams for the better solutions with respect to astigmatism, using a convergent incident wave ($\rho = -1000$ mm, case II) or a divergent incident wave ($\rho = 60$ mm, case III). The improvement is quite significant.

As can be seen from Figs. 10 and 11, the higher-order aberrations produce an asymmetric focal spot. Although the principal ray follows a straight line, the center of gravity of the spot deviates slightly. The ray-tracing results show that these deviations are less than ± 18 μm for a beam diameter of $D = 5$ mm and less than ± 8 μm for $D = 3$ mm.

The phase Φ is described up to second order by Eq. (51). The theory presented could be extended to higher order. Equations (52)–(54) show that in the direction of the scan line $\mathbf{x}(s)$ the solutions are completely determined by the first- and the second-order terms, whereas perpendicular to the scan line corrections by higher-order terms are still possible.

7. CONCLUSIONS

An analytical method to determine the phase function of a holographic optical scanning element that will generate a given line $\mathbf{y}(t)$ in space by a movement $\mathbf{x}(s)$ of the hologram has been developed. It turns out that in the direction of the scan line $\mathbf{x}(s)$ the solutions are completely determined by the first- and second-order derivatives, which describe the direction and the curvature of the outgoing wave. As a consequence, the displacement s of the hologram and the displacement t of the focal spot are related by the scan equation $t(s)$, which depends only on the scan geometry.

The application of the method described to specific scan problems is easily achieved by using the second-order (paraxial) approximation for the incident and the outgoing beams. In particular, the design of holographic scanners that generate straight lines $\mathbf{y}(t)$ in space by linear and by circular motions $\mathbf{x}(s)$ was studied in detail. It turns out that a circular motion cannot generate a straight line in space without producing astigmatism of the focal spot.

The higher-order aberrations of these second-order analytical solutions were examined with the help of geometrical ray tracing. Aberrations perpendicular to the scan direction can still be eliminated by appropriate corrections of the hologram phase function, whereas astigmatism and other higher-order aberrations, especially in the scan direction, cannot be removed completely. However, optimum numerical design methods could be used to improve further the solutions found by the analytical approach presented.

REFERENCES

1. H. Iwaoka and T. Shiozawa, "Aberration-free linear holographic scanner and its application to a diode-laser printer," Appl. Opt. **25,** 123–129 (1986).
2. M. Malin and H. E. Morrow, "Wavelength scaling holographic elements," Opt. Eng. **20,** 756–758 (1981).
3. O. Bryngdahl and W. Lee, "Laser beam scanning using computer-generated holograms," Appl. Opt. **15,** 183–194 (1976).
4. Y. Ono and N. Nishida, "Holographic laser scanners using generalized zone plates," Appl. Opt. **21,** 4542–4548 (1982).
5. G. T. Sincerbox, "Holographic scanners: applications, performance and design," in *Laser Beam Scanning*, Vol. 8 of Optical Engineering, G. F. Marshall, ed. (Dekker, New York, 1985), pp. 1–62.
6. Y. Ono and N. Nishida, "Holographic optical elements with optimized phase-transfer functions," J. Opt. Soc. Am. A **3,** 139–142 (1986).
7. K. A. Winick and J. R. Fienup, "Optimum holographic elements recorded with nonspherical wave fronts," J. Opt. Soc. Am. **73,** 208–217 (1983).
8. J. Kedmi and A. A. Friesem, "Optimized holographic optical elements," J. Opt. Soc. Am. A **3,** 2011–2018 (1986).
9. R. Dändliker, K. Hess, and T. Sidler, "Astigmatic pencils of rays reconstructed from holograms," Isr. J. Technol. **18,** 240–246 (1980).
10. W. T. Welford, "A vector raytracing equation for hologram lenses of arbitrary shape," Opt. Commun. **14,** 322–323 (1975).